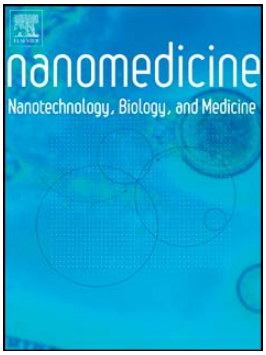

Ultrasound-activated piezoelectric P(VDF-TrFE) / boron nitride nanotube composite films promote differentiation of human SaOS-2 osteoblast-like cells

Giada Graziana Genchi, Edoardo Sinibaldi, Luca Ceseracciu, Massimiliano Labardi, Attilio Marino, Sergio Marras, Giorgio De Simoni, Virgilio Mattoli, Gianni Ciofani

PII: S1549-9634(17)30090-4
DOI: doi: 10.1016/j.nano.2017.05.006
Reference: NANO 1588

To appear in: *Nanomedicine: Nanotechnology, Biology, and Medicine*

Received date: 19 April 2017
Revised date: 10 May 2017
Accepted date: 10 May 2017

Please cite this article as: Genchi Giada Graziana, Sinibaldi Edoardo, Ceseracciu Luca, Labardi Massimiliano, Marino Attilio, Marras Sergio, De Simoni Giorgio, Mattoli Virgilio, Ciofani Gianni, Ultrasound-activated piezoelectric P(VDF-TrFE) / boron nitride nanotube composite films promote differentiation of human SaOS-2 osteoblast-like cells, *Nanomedicine: Nanotechnology, Biology, and Medicine* (2017), doi: 10.1016/j.nano.2017.05.006

Ultrasound-activated piezoelectric P(VDF-TrFE) / boron nitride nanotube composite films promote differentiation of human SaOS-2 osteoblast-like cells

Giada Graziana Genchi[a,*], *Edoardo Sinibaldi*[b,*], *Luca Ceseracciu*[c], *Massimiliano Labardi*[d], *Attilio Marino*[a,e], *Sergio Marras*[f], *Giorgio De Simoni*[g], *Virgilio Mattoli*[a], *Gianni Ciofani*[a,h,*]

[a]Istituto Italiano di Tecnologia, Smart Bio-Interfaces, Viale Rinaldo Piaggio 34, 56025 Pontedera (Pisa), Italy

[b]Istituto Italiano di Tecnologia, Center for Micro-BioRobotics @SSSA, Viale Rinaldo Piaggio 34, 56025 Pontedera (Pisa), Italy

[c]Istituto Italiano di Tecnologia, Smart Materials, Via Morego 30, 16163 Genova, Italy

[d]CNR-IPCF, c/o Physics Department, University of Pisa, Largo Pontecorvo 3, 56127 Pisa, Italy

[e]Scuola Superiore Sant'Anna, The BioRobotics Institute, Viale Rinaldo Piaggio 34, 56025 Pontedera (Pisa), Italy

[f]Istituto Italiano di Tecnologia, Nanochemistry Department, Via Morego 30, 16163 Genova, Italy

[g]CNR, Nanoscience Institute, NEST Laboratory, Piazza San Silvestro 12, I-56127 Pisa, Italy

[h]Polytechnic University of Turin, Department of Mechanical and Aerospace Engineering, Corso Duca degli Abruzzi 24, 10129 Torino, Italy

[*] Corresponding Authors

Giada Graziana Genchi, giada.genchi@iit.it

Edoardo Sinibaldi, edoardo.sinibaldi@iit.it

Gianni Ciofani, gianni.ciofani@iit.it

Istituto Italiano di Tecnologia

Viale Rinaldo Piaggio 34, 56025 Pontedera (Pisa), Italy

Tel. +39050883035

Fax +39050883497

Abstract word count: 115

Complete manuscript word count: 4643

Number of references: 45

Number of figures/tables: 6+2

Authors declare no conflict of interest.

Abstract

Piezoelectric films of poly(vinylidenedifluoride-trifluoroethylene) (P(VDF-TrFE)) and of P(VDF-TrFE) / boron nitride nanotubes (BNNTs) were prepared by cast-annealing and used for SaOS-2 osteoblast-like cell culture. Films were characterized in terms of surface and bulk features, and composite films demonstrated enhanced piezoresponse compared to plain polymeric films (d_{31} increased by ~80%). Osteogenic differentiation was evaluated in terms of calcium deposition, collagen I secretion, and transcriptional levels of marker genes (*Alpl*, *Col1a1*, *Ibsp*, and *Sparc*) in cells exposed or not to ultrasounds (US); finally, a numerical model suggested that the induced voltage (~20-60 mV) is suitable for cell stimulation. Although preliminary, our results are extremely promising and encourage the use of piezoelectric P(VDF-TrFE)/BNNT films in bone tissue regeneration.

Key-Words

P(VDF-TrFE); boron nitride nanotubes; piezoelectricity; ultrasounds; cell differentiation; bone.

Background

Piezoelectric materials are attracting increasing interest in several fields of regenerative medicine[1-3], including bone tissue engineering[4,5], as they can represent active implantable interfaces for electric stimulation delivery upon wireless mechanical stimulation, thus improving tissue regeneration/implant integration during crucial stages of healing[6-8].

It is indeed long known that bone tissue and its constituent collagen possess intrinsic piezoelectricity[9,10], and many piezoelectric materials have been tested to promote osteoregeneration both *in vitro* and *in vivo* with different degree of success, depending on both piezoelectric and mechanical properties[11-13]. Among them, some fluoropolymers, like poly(vinylidenedifluoride) (PVDF) and its copolymer with trifluoroethylene P(VDF-TrFE) are characterized by high biocompatibility, easy processability[14], and elevated piezoelectricity[8,15], nonetheless their mechanical properties make them poorly suitable to bone repair/regeneration. Some biocompatible nanoceramics are instead characterized by higher piezoelectricity and even better mechanical properties to the purpose: depending on the preparation method, boron nitride nanotubes (BNNTs) for instance may reach a Young's modulus of ~0.5-1.2 TPa[16,17]. Although much higher than that of bone tissue, this value can help to improve mechanical properties, for instance, of polymeric matrices. To date, only one example of BNNTs deposited in low amounts on glass coverslips and used as substrates for mesenchymal stem cell culture can be found in bone tissue engineering, demonstrating however that BNNTs significantly improved cell growth and osteogenic commitment in terms of alkaline phosphatase activity (AP, an early marker of osteodifferentiation) and production of osteocalcin (a late marker of osteodifferentiation)[18].

The use of BNNTs as second phase reinforcing (SPR) agents in complex matrices for bone tissue engineering has gradually started to emerge, demonstrating effectiveness of low amounts of nanomaterials to the mechanical property improvement in composites[19-21]. For

instance, polylactide–polycaprolactone composite films were prepared with 5% wt. BNNTs, determinining an increase in the Young's modulus and in the tensile strength by over 1000% and 100%, respectively. Tested with human osteoblasts (hOBs), these composites had no cytotoxic effects and significantly increased transcription of *Runx2* (an early marker of osteodifferentiation)[19]. BNNTs (4% wt.) were also used as SPR and grain refiner agents with hydroxyapatite, demonstrating an improvement of the Young's modulus by 120% and supporting human osteoblast viability[20].

Very few studies instead dynamically explored the potentialities of the mentioned piezoelectric materials and composites for bone regeneration: among them, there is a work on the interaction of PVDF with human adipose stem cells upon mechanical stimulation (vibrations)[22]. Moreover, great efforts have been deployed by our group to the investigation of piezoelectric materials as transducers of mechanical stimulation into electrical stimulation of different cell types[23,24], including osteoblasts. For instance, we fabricated 3D trabecular bone-mimicking scaffolds doped with barium titanate nanoparticles (BTNPs), and investigated their interaction with SaOS-2 osteoblast-like cells. Characterized by higher d_{33} piezoelectric coefficient compared to the non-doped substrates, BNTP-composite scaffolds promoted higher cell differentiation upon US application. In particular, Ki-67 expression, indicative of exit from cell cycle, was found to be significantly lower in cells cultured on composite scaffolds after US treatment, whereas collagen I and hydroxyapatite deposition was found to be significantly higher[7].

Due to the paucity of evidences in the literature concerning piezoelectric nanocomposites interacting with bone cells and exploiting direct piezoelectric effect for cell behavior tuning, here we prepared piezoelectric films with P(VDF-TrFE) and BNNTs, and studied their effects on human SaOS-2 cells. We primarily aimed at assessing the potentialities of BNNTs as second phase reinforcing agents in the preparation of polymer-based films for bone tissue

engineering. We also aimed at verifying whether the piezoelectric properties of the polymer-based films were improved by the addition of piezoelectric nanoceramic BNNTs. Finally, we aimed at investigating cell response after US stimulation to demonstrate that film mechanoelectric transduction is actually beneficial to osteogenic differentiation in terms of calcium deposition, transcription of differentiation markers and secretion of extracellular matrix proteins.

Methods

Film and cell culture system preparation

Poly(vinylidenedifluoride-trifluorethylene) (PVDF-TrFE, 70/30 mol/mol copolymer) from Piezotech (Pierre-Bénite, France) and boron nitride nanotubes (BNNTs) from BNNT LLC (Newport News, VA) were used for film preparation. BNNT are prepared by pressurized vapor/condenser (PVC) method, leaving residual hBN and amorphous particles, ~15% micro-droplets of elemental boron, and no catalyst impurities (data obtained from supplier).

For plain polymeric films, 1 g of P(VDF-TrFE) was dissolved in 10 ml of methylethylketone (MEK, Carlo Erba, Cornaredo, Italy) through a tip sonicator set at 8 W for 10 min. MEK was chosen for its higher safety for both operators and cell cultures compared to typical P(VDF-TrFE) solvents (dimethylacetamide and dimethylformamide). For composite films, 990 mg of P(VDF-TrFE) and 10 mg of BNNTs were used. First, BNNTs were sonicated for 10 min in 10 ml of MEK; then, P(VDF-TrFE) was added, and the mixture was sonicated for further 10 min. The mixtures were allowed to rest for 30 min prior to processing. Films were prepared by casting 1 ml of mixtures on Ibidi film pieces (2.8 cm x 5.6 cm, made of cyclic olefin copolymer) and annealing at 40°C on a hot plate for 4 h. The residual solvent was removed by storing samples under vacuum for 12 h. Prior to film characterization and cell culture, samples were cut into 20 mm side squares and exposed to O_2 plasma (25 sccm, 50 W, 120 s,

0.5 mbar in a Colibrì reactor, Gambetti, Binasco, Italy) to increase surface hydrophilicity. Then, they were anchored to the center of 35 mm diameter Petri dishes through a layer of adhesive poly(dimethylsiloxane) (Sylgard 184, Dow Corning, Midland, MI) of 1 mm in height, that was sterilized by UV exposure for 30 min. After exposure to plasma and positioning on PDMS, films were sterilized by incubation with 100 U/ml penicillin / 100 µg/ml streptomycin (Gibco, Waltham, MA) in phosphate buffered saline (PBS, Gibco) for 1 h.

Electron microscopy

BNNTs deposited on a lacey carbon-copper grid were observed on a JEM 1011 transmission electron microscope (TEM, JEOL, Akishima, Japan) working at 100 kV. Diffraction patterns of the nanotubes were also acquired on the same equipment through a Selected Area Electron Diffraction (SEAD) lens. All images and patterns were acquired with a Gatan Orius CCD camera. Films were characterized with a JEOL JSM-7500F scanning electron microscope (SEM) equipped with a cold FEG working at 5 kV. Prior to imaging, films were immersed into liquid nitrogen and then bended to obtain a clean fracture surface. Carbon-coating was deposited before imaging (evaporation time: 2800 ms *per* pulse; 3 pulses; coating thickness: ~15 nm).

Piezoelectric characterization

Surface topography was mapped with a Multimode atomic force microscope (AFM Instruments, Veeco, Plainview, NY) equipped with a Nanoscope IIIa controller. For tapping mode AFM, non-contact mode silicon cantilevers were used (Veeco RTESP10, with 265-311 kHz nominal resonant frequency, and 20-80 N/m nominal spring constant). The same instrument was operated as a piezoresponse force microscope (PFM) in contact-resonance

mode[25], by using contact mode silicon cantilevers with 14 kHz nominal resonant frequency and 0.2 N/m nominal spring constant (Arrow-Cont NanoWorld, Neuchâtel, Switzerland).

Piezoelectric transduction was measured on films cut into stripes of 20 mm x 5 mm x 0.08 mm (*xyz*), by loading into a home-made setup briefly described hereafter. One end of the sample was fixed to a holder, attached to a harmonic steel slab spring through Teflon clamps. The other end was attached to a microtranslator enabling sample pre-tension. An electric potential was applied in transverse direction (*z*) through a pair of metal slabs, positioned very close to the stripe surface (*xy*). The transverse electric field produced a longitudinal deformation (along *x*) with magnitude proportional to the piezoelectric coefficient d_{31} of the material. Alternating electrical drive at the spring resonance frequency produced a ~20-fold enhancement of vibration. Bending of the steel slab was detected by the optical lever method. The converse piezoelectric coefficient d_{31} was then calculated as specified elsewhere[25], whereas g_{31} and e_{31} were derived as:

$$g_{31} = \frac{d_{31}}{\varepsilon_r \cdot \varepsilon_0} \quad (1)$$

$$e_{31} = d_{31} \cdot E_Y \quad (2)$$

where ε_0 is the dielectric permittivity of vacuum, ε_r is the relative dielectric constant of the material (~8)[26], and E_Y is the Young's modulus.

Cell proliferation

SaOS-2 osteosarcoma cells (European Collection of Authenticated Cell Lines 89050205) were cultured with proliferation medium: high glucose Dulbecco's Modified Eagle's Medium (DMEM, Gibco), added with 10% fetal bovine serum (FBS, Gibco), 2 mM L-glutamine (Gibco), 1 mM sodium pyruvate (Gibco), 2.5 µg/ml amphoterycin B (Sigma Aldrich, Saint

Louis, MO), and 100 U/ml penicillin-100 μg/ml streptomycin (Gibco). For proliferation studies, 10,000 cells/cm^2 were seeded on P(VDF-TrFE) and on P(VDF-TrFE)/BNNT films. Ibidi film squares were used as non-piezoelectric controls. Proliferation medium volume was 2 ml for each Petri dish. Methods for investigating proliferative behavior and the relative results are presented in Supplemental Materials.

Cell differentiation

For differentiation studies, 10,000 cells/cm^2 were seeded on all substrates. Adhesion was allowed for 48 h before administration of differentiation medium: low glucose DMEM (Gibco), 10% FBS, 10 mM β-glycerophosphate disodium salt hydrate (Sigma Aldrich), 50 μM L-ascorbic acid (Sigma Aldrich), 100 nM dexamethasone (Sigma Aldrich D4902), 2.5 μg/ml amphoterycin B (Sigma Aldrich), and 100 U/ml penicillin / 100 μg/ml streptomycin. For the whole study, cells were incubated at 37°C in a 5% CO_2 humidity saturated atmosphere, and cell culture medium was changed every two days. Differentiation was allowed for 7 days.

Cell stimulation

Mechanical stimulation was provided twice a day for 10 s during cell differentiation. Ultrasounds (US) were applied with a Sonopore K-TAC 4000 device (Sonidel, Raheny, Ireland) by setting 1 W/cm^2, 100 Hz burst rate, and 100% duty cycle. A KP-S20 probe (20 mm diameter, covered with a thin layer of US gel) was put into adherent contact with the bottom of Petri dishes hosting cell cultures. Relative motions between the lid and the Petri dish bottom over the stimulation period were prevented with Parafilm sealing.

Alizarin Red staining

At the end of the differentiation period, cells were washed with Ca^{2+}/Mg^{2+} added-phosphate buffered saline (PBS, Gibco). Fixation was performed as specified before, then cells were

stained by incubation with Alizarin Red (Millipore, Billerica, MA) for 30 min. After five rinses with ultrapure water, the cultures were imaged: for each sample, 10 images were acquired, and the percentage of areas stained with Alizarin Red was semi-automatically analyzed with ImageJ software.

Quantitative real-time reverse transcriptase polymerase chain reaction (qRT-PCR)

At the end of the differentiation period, RNA extraction was performed by using the RNeasy® Plus Micro kit (Qiagen, Venlo, the Netherlands) in the QIAcube robotic workstation (Qiagen). First, cells were disrupted with RLT lysis buffer added with 0.14 M β-mercaptoethanol, then the lysates were manually loaded on purification columns and finally the automated purification protocol was run. The obtained RNA was analyzed by quantification of absorbance at 230, 260 and 280 nm with a NanoDrop spectrophotometer (Thermo Scientific, Waltham, MA). Afterwards, 300 µg of total RNA were reverse-transcribed into cDNA by using 1X iScript™ Reverse Transcription Supermix (Bio-Rad, Hercules, CA) and by applying the following thermal protocol with a CFX Connect™ Real-Time PCR Detection System (Bio-Rad): priming at 25°C for 5 min, reverse transcription at 42°C for 30 min, and reverse transcriptase inactivation at 85°C for 5 min. The obtained cDNA was then 10-fold diluted with ultrapure water and used for amplification. For each reaction, 10 µl of SsoAdvanced™ SYBRGreen® Supermix (Bio-Rad), 1 µl of forward and reverse primers (8 µM), 4 µl of ultrapure water, and 5 µl of diluted cDNA were mixed. The following thermal protocol was applied: one cycle at 98°C for 30 s, 40 cycles at 98°C for 3 s and 60°C for 15 s, then a temperature ramp from 65°C to 95°C with 0.5°C/s increments. The latter was set in order to obtain melting curves and thus exclude unspecific amplifications. Relative fold expression was calculated by using *Ldha* as reference gene and by using the $\Delta\Delta Ct$ method. Primer sequences (reported in Supplemental Materials) of *Alpl*, *Col1a1*, *Ibsp*, and *Sparc* were

obtained from[6], whereas sequence of *Ldha* was obtained with "Pick Primers" tool on Pubmed.

Statistical analysis

Normality of the data distribution was investigated with Shapiro-Wilk test; then, one-way ANOVA followed by HSD *post-hoc* test was performed. Quantitative RT-PCR results were evaluated with Bio-Rad CFX Manager software. In all experiments, statistical significance was set at 5% (* stands for $p < 0.05$, ** for $p < 0.01$ and *** for $p < 0.001$).

Numerical modeling: estimate of the voltage induced during cell stimulation

An extensive quantitative control of all the working parameters involved in the stimulation experiments was beyond the scope of the present study. Nevertheless, aiming at estimating the voltage induced on the film by US to support the interpretation of the stimulation experiments in terms of piezoelectric effects, we introduced a numerical model based on the literature. In particular, by considering the reduced film thickness ($t_f = 50$ μm) compared to the characteristic length-scale of the experimental setup, a simplified two-step approach was implemented. The US-induced pressure field was first computed by neglecting the film; the voltage was then derived for the plain polymeric films based on an additional piezoelectric coefficient (namely g_{33}) available in literature. The considered steps (including, in particular, the governing equations) are described in the Supplementary Materials.

Results

Film characterization

A TEM image of BNNTs is presented in Figure 1A. BNNTs were imaged after sonication in MEK for 10 min. BNNTs appear as bundles of multi-walled tubes with 10 nm average diameter and lengths on the micrometer size (see Supplementary Materials for a low

magnification TEM image of BNNTs). Figure 1B represents the nanotube diffraction pattern and Figure 1C depicts the relative indexes, showing correspondence to the hexagonal cell of boron nitride[27]. Figure 1D shows a TEM image of the composite film bulk, characterized by curvilinear electron-lucent regions ascribable to BNNTs. Figure 1E and 1F report the SEM images of the film fracture surfaces. Figure 1E shows a neat fracture surface in a plain P(VDF-TrFE) film, whereas Figure 1F displays a highly patterned fracture surface in a P(VDF-TrFE)/BNNT film, that can be ascribed to partial pull-out of BNNTs from the matrix.

Figures 2A and 2B represent the AFM topographic maps of the P(VDF-TrFE) and of the P(VDF-TrFE)/BNNT films, respectively. These maps were used to derive the root mean square roughness of the surface, that was ~30 nm for both substrates. Figures 2C and 2D represent the PFM maps of the same films. The composite film shows a higher average piezoresponse compared to the plain polymeric one, owing to the presence of BNNTs.

Necessary to piezoelectric coefficient calculations, mechanical characterization results of the films are presented and discussed in Supplementary Materials.

The results of the piezoelectric property measurements with home-made set up are reported in Table 1. The converse piezoelectric coefficient d_{31} was 6 pm/V for P(VDF-TrFE) film (in full agreement with[26]) and 11 pm/V for P(VDF-TrFE)/BNNT films. The direct piezoelectric coefficient g_{31} was 0.085 V·m/N for P(VDF-TrFE) and 0.155 V·m/N for P(VDF-TrFE)/BNNT films, whereas the effective transverse piezoelectric coefficient e_{31} was 1.92 mC/m^2 for P(VDF-TrFE) and 7.59 mC/m^2 for P(VDF-TrFE)/BNNT films. Ibidi film was used as control (a weak response was nonetheless induced because of the relatively strong fields involved in the measurement).

X-ray diffraction patterns and differential scanning calorimetry thermograms of P(VDF-TrFE) and P(VDF-TrFE)/BNNT films are reported in Supplementary Materials, showing peaks only related to α and β phases of P(VDF-TrFE) in both film typologies.

Cellular response

Optical microscopy images of SaOS-2 cells stained with Alizarin Red after 7 days of differentiation either in the absence or the presence of US stimulation are reported in Figure 3A. These images qualitatively show that Alizarin Red stained areas are comparable on all substrates in the absence of US, whereas they are larger on P(VDF-TrFE)/BNNT films after US stimulation with respect to the other substrates. Image analysis aiming at the quantification of the Alizarin Red stained areas confirmed these results. As shown in Figure 3B, the percentage of Alizarin Red stained areas on P(VDF-TrFE)/BNNT films after US stimulation is significantly higher than that one of cultures on all substrates and not stimulated with US ($p < 0.001$). This percentage is also significantly higher than that one on control films ($p < 0.05$) and than that one on P(VDF-TrFE) films ($p < 0.01$) after US stimulation. The percentages of Alizarin Red stained areas indeed were 1.3 ± 0.4 for Ibidi films, 1.1 ± 0.6 for P(VDF-TrFE) films and 3.2 ± 0.8 for P(VDF-TrFE)/BNNT films without US stimulation. The percentages of Alizarin Red stained areas instead were 0.9 ± 0.5 for Ibidi films, 1.9 ± 0.6 for P(VDF-TrFE) films and 5.7 ± 3.3 for P(VDF-TrFE)/BNNT films with US stimulation.

Transcriptional levels of osteogenic differentiation markers are shown in Figure 4 (with cultures on Ibidi films not treated with US considered as control for normalization). Interestingly, the markers were significantly up-regulated in cells cultured on composite films and exposed to US compared to the control.

Alkaline phosphatase gene (*Alpl*) underwent a 1.4-fold down-regulation in SaOS-2 cultured on P(VDF-TrFE) films without US stimulation ($p < 0.01$), while a 1.4-fold down-regulation and a 1.4-fold up-regulation in cells cultured on control and P(VDF-TrFE)/BNNT films with US stimulation, respectively ($p < 0.01$).

Collagen I gene (*Col1a1*) was 1.2-fold down-regulated in SaOS-2 cultured on P(VDF-TrFE) films without US stimulation ($p < 0.05$). It also underwent a 1.8-fold down-regulation in cells cultured on control films with US stimulation ($p < 0.001$). *Col1a1* was up-regulated by 1.1-folds in SaOS-2 cultured on P(VDF-TrFE) films with US stimulation ($p < 0.05$) and by 1.8-folds in cells cultured on P(VDF-TrFE)/BNNT film with US stimulation ($p < 0.001$).

Integrin binding sialoprotein gene (*Ibsp*) underwent a 1.4- and a 2.3-fold up-regulation in SaOS-2 cells cultured on P(VDF-TrFE)/BNNT films without and with US stimulation, respectively ($p < 0.01$).

Secreted protein acidic and rich in cysteine (osteonectin) gene (*Sparc*) underwent a 1.3-fold down-regulation in SaOS-2 cultured on P(VDF-TrFE) films without US stimulation. This marker was also up-regulated by 1.6- and 2.7-folds in cells cultured on P(VDF-TrFE) and on P(VDF-TrFE)/BNNT films with US stimulation, respectively ($p < 0.001$).

Fluorescence microscopy images of SaOS-2 cells immunostained for collagen I (COL1) detection after 7 days of differentiation either in the absence or the presence of US stimulation are reported in Figure 5A. These images qualitatively show that COL1-positive areas are comparable on all substrates in the absence of US, whereas they increase on P(VDF-TrFE) and P(VDF-TrFE)/BNNT films after US stimulation with respect to the control substrates. These results were quantitatively confirmed by image analysis, that demonstrated a significantly higher secretion of COL1 on piezoelectric substrates (compared to the control) only after US stimulation (Figure 5B, $p < 0.001$). Moreover, the US-exposed composite films

promoted the highest deposition of COL1 ($p < 0.001$). The percentages of COL1-positive area were 20.4 ± 5.1 on Ibidi, 17.0 ± 0.5 on P(VDF-TrFE), and 16.7 ± 2.6 on (PVDF-TrFE)/BNNT films not exposed to US, whereas they were 17.9 ± 1.6 on Ibidi, 47.6 ± 11.2 on P(VDF-TrFE), and 72.0 ± 7.8 on (PVDF-TrFE)/BNNT films exposed to US.

Estimate of the voltage induced during cell stimulation

The amplitude of the pressure variation induced at the film site is reported in Figure 6A. Besides considering the uncertainty on the sound speed within PDMS (c_{PDMS}), it illustrates pressure sensitivity to d_{US}. Model implementation was performing enough to allow for a cheap *in silico* exploration of the considered working domain: a batch of nearly 1000 simulations launched by interfacing Matlab (www.mathworks.com) with Comsol took less than 20 h on a common desktop PC. For the measured d_{US} value, the amplitude of the pressure variation resulted to be 2-6 kPa. The corresponding voltage induced on P(VDF-TrFE) films (reported in Figure 6B) resulted to be 23-61 mV.

Discussion

In this work we demonstrated that SaOS-2 osteoblast-like cell differentiation was promoted by P(VDF-TrFE)/BNNT films upon application of US owing to the direct piezoelectric effect. In particular, we demonstrated that the addition of a very low amount (1%) of nanotubes to the polymeric matrix was effective at improving piezoelectric properties of films compared to the polymeric ones, while leaving comparable surface topography and improving the Young's modulus.

Measurements of the piezoelectric behavior of the films evidenced that the transverse piezoelectric coefficient d_{31} of the films underwent a 1.8-fold increase by addition of BNNTs to P(VDF-TrFE). This translated in a likewise increase of the direct piezoelectric coefficient g_{31}, whereas e_{31} underwent a 3.9-fold increase. Considering the standard deviation of the

angle formed by the BNNT axis with respect to the direction of piezoelectric measurement, prior studies suggested that BNNT dispersion can be sufficient to motivate the observed piezoresponse, even for a non-piezoelectric polymer such as polyimide[28]. However, the related physical mechanism remains unclear[28], and the fact that BNNT piezoelectricity per se is still not completely understood[29] makes it very hard, at present, to put forward any explanations for underlying physical phenomena in composites. Moreover, it has also been reported that dopant nanoparticles can facilitate the alignment of the dipole direction, and thus the depolarization of the whole film, even in absence of directs effects on the crystalline structure of the polymer, as shown by XRD analysis.[30]

This is in agreement with PFM investigations on the same samples. Although PFM is an effective method for the measurement of local piezoelectric response on stiff materials[25], its application to polymers may only provide a qualitative description of piezoelectric effects distribution on a surface. PFM maps in Figure 2C and 2D show the surface piezoelectric response quantified in the same units of the longitudinal piezoelectric coefficient d_{33} (pm/V) and that is not comparable to the bulk d_{33} in the case of soft samples. A higher average piezoresponse is observed for the composite film (Figure 2D), while both maps show lamellar regions of increased response, that could be ascribed to the crystalline fraction of P(VDF-TrFE) since they are present also on the sample of pure polymer (Figure 2C) and their density does not seem compatible with the low concentration of BNNTs.

To benchmark the potential of composite films as future bone augmenting biomaterials, the values of some piezoelectric coefficients were gathered from the literature and reported in Table 2, related to bone and its constituents collagen and hydroxyapatite, as well as poly(L-lactic acid), pristine BNNTs and pristine P(VDF-TrFE)[12,31-37]. Amongst the materials in Table 2, described by only mentioning the d_{ij} coefficients for consistency, PZT stands out for its relative magnitude; however, its use for biomedical purposes is hampered by the related

toxic effects[38], whence the quest for more biocompatible piezoelectric biointerfaces. For bone calcification purposes it may useful to consider the piezoelectric coefficient *e*, since it gives a direct measure of how much charge would be available *per* unit area during calcification. Noticeably, BNNT integration dramatically raised the *e* coefficient compared to plain films. This further supports the potential of BNNT integration to foster calcification.

Differentiation of SaOS-2 cells in terms of calcium deposition was significantly improved by P(VDF-TrFE)/BNNT films and US with respect to all of the substrates, both exposed or not-exposed to US. This demonstrates the beneficial effects of BNNT addition to the polymeric matrix of the films (even in low quantity), but also underlines the importance of the synergistic mechanical stimulation to improving calcium deposition. The investigation on the transcriptional levels of osteodifferentiation marker genes demonstrated up-regulation on composite films (compared to the control substrates) in cultures stimulated with US. This represents a neat evidence of the biological response evoked by the direct piezoelectric effect of the films upon US exposure. The markers were also up-regulated on P(VDF-TrFE)/BNNT films in comparison to P(VDF-TrFE) films, thus demonstrating that the higher piezoelectric properties of the composite films with respect to the plain polymeric ones were more effective at eliciting stronger cellular responses also at a transcriptional level.

Of the genes considered in our study, *Alpl* and *Col1a1* are early markers of osteoblast differentiation[6]. *ALPL* plays a fundamental role in extracellular matrix mineralization by locally increasing the concentration of phosphate (mineralization promoter), whereas *COL1A1* is the most abundant protein in the organic component of bone extracellular matrix. *Col1a1* is normally expressed at low levels in SaOS-2 cells[39]. In our experiment, *Alpl* and *Col1a1* transcription was up-regulated on composite films after US stimulation, thus demonstrating the importance of the direct piezoelectric effect of P(VDF-TrFE)/BNNT films

in tuning cellular responses. Interestingly, the relative expression of *Alpl* was comparable to that one of *Col1a1*.

Typically, *Alpl* transcription declines as osteodifferentiation proceeds, while the transcription of other genes, such as *Sparc*[40], is up-regulated. *SPARC* promotes osteoblast commitment and accomplishes both structural and regulatory duties during bone development and repair[41]. Very interestingly, *Sparc* transcription was up-regulated in cultures on composite films and exposed to US, and the level of up-regulation was much higher that that one found for *Alpl*. This suggests the achievement of a more advanced differentiated status in SaOS-2 cells cultured on P(VDF-TrFE)/BNNT films and stimulated with US compared to the other films, even after exposure to US.

Very relevant to bone tissue engineering is the transcriptional level of *Ibsp*. The latter is another late marker of osteoblast differentiation[42] which induces hydroxyapatite nucleation and has highest transcriptional levels in association to *de novo* bone formation[42]. In our experiment, this was the marker that demonstrated the highest up-regulation, thus reinforcing the evidences on the other markers of differentiation.

Overall, our results on transcriptional levels of differentiation markers suggest that P(VDF-TrFE)/BNNT composite films in tight synergy with US accelerate the maturation of SaOS-2 cells in comparison to the other substrates, anticipating the transcription of late markers of osteogenic differentiation. To the best of our knowledge, our study represents the first wider investigation on osteodifferentiation markers on piezoelectric polymer/BNNT composite films at a transcriptional level[19]. Further, our study provides preliminary evidences of a significant improvement of SaOS-2 differentiation even at phenotype level that confirm data obtained at a transcriptional level, by showing increasing COL1 secretion on P(VDF-TrFE) < P(VDF-TrFE)/BNNT films exposed to US. We deem that BNNT dispersion in the polymeric

matrix increases its piezoelectricity above a certain threshold for the biological responses to be suitably triggered/tuned.

Concerning the voltage induced through US, the numerical results confirmed that it was high enough for effectively stimulating cells. The model was grounded on some simplifications. In particular, by neglecting nonlinear wave propagation effects and transport in the Petri wall, we could have introduced some uncertainty in the pressure field computation, yet without corrupting its order of magnitude[43], as functional to the sought estimate. On the other hand, we accurately controlled the position of the reflecting liquid/air interface, which also plays a key role in the computation of the pressure field[43] (due to the potential occurrence of resonances that we also explored through auxiliary, supporting simulations). Hence, despite the high sensitivity of US exposure to the many involved working parameters[44], and in spite of the further approximation introduced for computing the induced voltage, our numerical results were commensurate with model aim, and they positively complemented the other experiments. Lacking a measured g_{33} value for P(VDF-TrFE)/BNNT composite films, we could only provide an estimate for P(VDF-TrFE) films; nevertheless, the obtained voltage was already high enough to effectively elicit cell response[45]. Combining this result with the enhanced piezoelectric properties of composite films compared to plain polymeric ones, we attribute the larger improvement provided by US to the composite films to an even higher voltage induced by BNNT loading. This supports composite film use for improving piezoelectric cell stimulation.

To conclude, preliminary evidences of enhanced differentiation of SaOS-2 osteoblast-like cells were found on composite piezoelectric films prepared with P(VDF-TrFE) and BNNTs upon ultrasound stimulation. Other investigations are necessary, in particular at later time points and at a translational level, aiming at assessing and possibly confirming the extent of expression of late differentiation markers. Further, exploring the direct piezoelectric effect

exerted by P(VDF-TrFE)/BNNT films with primary cells is mandatory for any realistic application of the proposed materials, for instance as patches or coatings, in bone tissue engineering.

Acknowledgements

Alice Scarpellini and Doriana Debellis (IIT) are gratefully acknowledged for technical assistance with SEM and TEM imaging. Serena Danti (University of Pisa) is kindly acknowledged for motivating the development of the experimental setup for transverse piezoelectric coefficient measurements on soft samples.

Figure and Table captions

Figure 1. Transmission electron microscopy (TEM) image of BNNTs after sonication (A), X-ray diffraction pattern (B) and relative indexes (C). TEM image of the P(VDF-TrFE)/BNNT film showing curvilinear electron-lucent regions in the matrix ascribable to BNNTs (D). Scanning electron microscopy images of the fracture surface of cryofractured P(VDF-TrFE) (E) and of P(VDF-TrFE)/BNNT film (F).

Figure 2. Atomic force microscopy images of P(VDF-TrFE) (A) and P(VDF-TrFE)/BNNT films (B). Piezoresponse force microscopy maps of P(VDF-TrFE) (C) and P(VDF-TrFE)/BNNT films (D).

Figure 3. Bright field microscopy images of Alizarin Red stained SaOS-2 cells after culture on Ibidi (as control substrate), P(VDF-TrFE) and P(VDF-TrFE)/BNNT films for 7 days under differentiative conditions, either in the absence or in the presence of ultrasounds (US) (A). Quantification of the percentage of Alizarin Red stained areas, performed on bright field microscopy images (B). (* $p < 0.05$; ** $p < 0.01$; and *** $p < 0.001$)

Figure 4. Transcriptional analysis of osteogenic differentiation markers: alkaline phosphatase (*Alpl*); collagen I (*Col1a1*); integrin binding sialoprotein (*Ibsp*); and secreted protein acidic and rich in cysteine (*Sparc*) genes. Analysis was performed with qRT-PCR on cells cultured on Ibidi (as control), P(VDF-TrFE) and P(VDF-TrFE)/BNNT films for 7 days under differentiative conditions, either in the absence or in the presence of US stimulation (* $p < 0.05$; ** $p < 0.01$; and *** $p < 0.001$).

Figure 5. Fluorescence microscopy images of immunostained collagen I in SaOS-2 cell cultures on Ibidi (as control substrate), P(VDF-TrFE) and P(VDF-TrFE)/BNNT films after 7 days under differentiative conditions, either in the absence or in the presence of ultrasounds

(US) stimulation (A). Quantification of the percentage of collagen I stained areas, performed on fluorescence microscopy images (B) (* $p < 0.05$; ** $p < 0.01$; and *** $p < 0.001$).

Figure 6. Numerical results: amplitude of the pressure variation induced by ultrasounds at the film site (A); corresponding voltage for P(VDF-TrFE) films (B). Uncertainty on the sound speed within PDMS (c_{PDMS}) is accounted for by the corresponding variation in both plots; sensitivity to the Petri oscillation amplitude (d_{US}) is reported in (A).

Table 1. Piezoelectric characterization of P(VDF-TrFE) and P(VDF-TrFE)/BNNT films, with Ibidi film as negative control.

Table 2. Piezoelectric coefficient values of selected natural and synthetic materials.

References

1. Ciofani G, Danti S, Genchi GG, Mazzolai B, Mattoli V. Boron Nitride Nanotubes: Biocompatibility and Potential Spill-Over in Nanomedicine. *Small* 2013;9:1672-1685.

2. Genchi GG, Marino A, Rocca A, Mattoli V, Ciofani G. Barium titanate nanoparticles: Promising multitasking vectors in nano medicine. *Nanotechnology* 2016;**27**:232001.

3. Fernandez-Yague MA, Larrañaga A, Gladkovskaya O, Stanley A, Tadayyon G, Guo Y *et al.* Effects of Polydopamine Functionalization on Boron Nitride Nanotube Dispersion and Cytocompatibility. *Bioconjugate Chem* 2015;**26**:2025-2037.

4. Vanék P, Kolská Z, Luxbacher T, García JAL, Lehocký M, Vandrovcová M *et al.* Electrical activity of ferroelectric biomaterials and its effects on the adhesion, growth and enzymatic activity of human osteoblast-like cells. *J Phys D: Appl Phys* 2016;**49**:17.

5. Zhang X, Zhang C, Lin Y, Hu P, Shen Y, Wang K *et al.* Nanocomposite Membranes Enhance Bone Regeneration Through Restoring Physiological Electric Microenvironment. *ACS Nano* 2016;**10**:7279-7286.

6. Griffin M, Sebastian A, Colthurst J, Bayat A. Enhancement of Differentiation and Mineralisation of Osteoblast-like Cells by Degenerate Electrical Waveform in an In Vitro Electrical Stimulation Model Compared to Capacitive Coupling. *PLoS ONE* 2013:**8**,e72978.

7. Marino A, Barsotti J, de Vito G, Filippeschi C, Mazzolai B, Piazza V *et al.* Two-Photon Lithography of 3D Nanocomposite Piezoelectric Scaffolds for Cell Stimulation. *ACS Appl Mater Interfaces* 2015;**7**:25574-25579.

8. Rajabi AH, Jaffe M, Arinzeh TL. Piezoelectric materials for tissue regeneration: A review. *Acta Biomater* 2015;**24**:12-23.

9. Fukada E. Piezoelectricity and Electrostimulation in Bone. In: Tofail SAM and Bauer J, editors. *Electrically Active Materials for Medical Devices*, London, Imperial College Press, 2016, p. 19-28.

10. Fernandez-Yague MA, Vallejo-Giraldo C, Aceret GO, Pandit A, Biggs MJ. Biological Activity on Piezoelectric PVDF. In: Tofail SAM and Bauer J, editors. *Electrically Active Materials for Medical Devices*, London, Imperial College Press, 2016, pp. 167-176.

11. Teng NC, Nakamura S, Takagi Y, Yamashita Y, Ohgaki M, Yamashita K. A new approach to enhancement of bone formation by electrically polarized hydroxyapatite. *J Dent Res* 2001,**80**:1925-1929.

12. Gandhi AA, Wojtas M, Lang SB, Kholkin AL, Tofail SAM. Piezoelectricity in Poled Hydroxyapatite Ceramics. *J Am Ceram Soc* 2014,**97**:2867-2872.

10. Sadat-Shojai M. Electrospun Polyhydroxybutyrate/Hydroxyapatite Nanohybrids: Microstructure and Bone Cell Response. *J Mater Sci Technol* 2016,**32**:1013-1020.

14. Biggs MJP, Capdevila EP, Valejo-Giraldo C, Wind SJ. Cellular Response to Ferroelectric PVDF-TrFE Nanoscale Surfaces Formed by Varying Polymer Concentration. *Pharm Nanotechnol* 2014;**1**:42-48.

15. Martins P, Lopes AC, Lanceros-Mendez S. Electroactive phases of poly(vinylidene fluoride): Determination, processing and applications. *Prog Polym Sci* 2014;**39**:683-706.

16. Chopra NG, Zettl A. Measurement of the Elastic Modulus of a Multi-wall Boron Nitride Nanotube. *Solid State Commun* 1998;**105**:297-300.

17. Golberg D, Bando Y, Huang Y, Terao T, Mitome M, Tang C *et al.* Boron Nitride Nanotubes and Nanosheets. *ACS Nano* 2010;**4**:2979-2993.

18. Li X, Wang X, Jiang X, Yamaguchi M, Ito A, Bando Y *et al.* Boron nitride nanotube-enhanced osteogenic differentiation of mesenchymal stem cells. *J Biomed Mater Res Part B* 2015;**00B**:323-329.

19. Lahiri D, Rouzaud F, Richard T, Keshri AK, Bakshi SR, Kos L *et al.* Boron nitride nanotube reinforced polylactide–polycaprolactone copolymer composite: Mechanical properties and cytocompatibility with osteoblasts and macrophages in vitro. *Acta Biomater* 2010;**6**:3524-3533.

20. Lahiri D, Singh V, Benaduce AP, Seal S, Kos L, Agarwal A. Boron nitride nanotube reinforced hydroxyapatite composite: Mechanical and tribological performance and in-vitro biocompatibility to osteoblasts. *J Mech Behav Biomed Mater* 2011;**4**:44-56.

21. Farshid B, Lalwani G, Mohammadi MS, Simonsen J, Sitharaman B. Boron nitride nanotubes and nanoplatelets as reinforcing agents of polymeric matrices for bone tissue engineering. *J Biomed Mater Res Part B* 2017;**105**:406-419.

22. Ribeiro C, Pärssinen J, Sencadas V, Correia V, Miettinen S, Hytönen VP *et al.* Dynamic piezoelectric stimulation enhances osteogenic differentiation of human adipose stem cells. *J Biomed Mater Res Part A* 2015;**103A**:2172-2175.

23. Ciofani G, Danti S, D'Alessandro D, Ricotti L, Moscato S, Bertoni G *et al.* Enhancement of neurite outgrowth in neuronal-like cells following boron nitride nanotube-mediated stimulation. *ACS Nano* 2010;**4**:6267-6277.

24. Genchi GG, Ceseracciu L, Marino A, Labardi M, Marras S, Pignatelli F *et al.* P(VDF-TrFE)/$BaTiO_3$ Nanoparticle Composite Films Mediate Piezoelectric Stimulation and Promote Differentiation of SH-SY5Y Neuroblastoma Cells. *Adv Healthc Mater* 2016;**5**:1808-1820.

25. Labardi M, Likodimos V, Allegrini M. Force-microscopy contrast mechanisms in ferroelectric domain imaging. *Phys Rev B* 2000;**61**:14390.

26. Piezoelectric films technical information. Technical document by Piézotech S.A.S; available online at http://www.piezotech.fr/image/documents/22-31-32-33-piezotech-piezoelectric-films-leaflet.pdf (last accessed: 03/27/2017).

27. Gao S-P. Crystal structures and band gap characters of h-BN polytypes predicted by the dispersion corrected DFT and GW method. *Solid State Commun* 2012;**152**:1817-1820.

28. Kang J-H, Sauti G, Park C, Yamakov VI, Wise KE, Lowther SE, Fay CC, Thibeault SA, Bryant RG. Multifunctional electroactive nanocomposites based on piezoelectric boron nitride nanotubes *ACS Nano* 2015;**9**:11942-11950.

29. Tiano A L, Park C, Lee J W, Luong H H, Gibbons L J, Chu S-H *et al.* Boron nitride nanotube: synthesis and applications. *Proc. SPIE Nanosensors, Biosensors, and Info-Tech Sensors and Systems* 2014;**9060**:906006

30. Paik H, Choi Y-Y, Hong S, No K. Effect of Ag nanoparticle concentration on the electrical and ferroelectric properties of Ag/P(VDF-TrFE) composite films. *Sci Rep.* 2015; **5**:13209.

31. Anderson JC, Eriksson C. Electrical properties of dry and wet bone. *Nature* 1970;**227**:491-492.

32. Halperin C, Mutchnik S, Agronin A, Molotskii M, Urenski P, Salai M, Rosenman G. Piezoelectric Effect in Human Bones Studied in Nanometer Scale. *Nano Letters* 2004;**4**:1253-1256.

33. Fukada E. History and Recent Progress in Piezoelectric Polymers. *IEEE Trans Ultrason Ferroelect Freq Control* 2000;**47**:1277-1290.

34. Minary-Joland M, Yu MF. Nanoscale characterization of isolated individual type I collagen fibrils: polarization and piezoelectricity. *Nanotechnology* 2009;**20**:085706.

35. Ochiai T, Fukada E. Electromechanical Properties of Poly-L-Lactic Acid. *Jpn J Appl Phys* 1998;**37**:3374-336.

36. Akedo J, Lebedev M. Piezoelectric properties and poling effect of Pb(Zr, Ti)O_3 thick films prepared for microactuators by aerosol deposition. *Appl Phys Lett* 2000;**77**:1710-1712.

37. Nakhmanson SM, Calzolari A, Meunier V, Bernholc J, Buongiorno Nardelli M, Spontaneous polarization and piezoelectricity in boron nitride nanotubes, *Phys Rev B* 2003;**67**:235406.

38. Saito Y, Takao H, Tani T, Nonoyama T, Takatori K, Homma T *et al.* Lead-free piezoceramics. *Nature* 2004;**432**:84-87.

39. Mayr-Wohlfart U, Fiedler J, Günther KP, Puhl W, Kessler S. Proliferation and differentiation rates of a human osteoblast-like cell line (SaOS-2) in contact with different bone substitute materials. *J Biomed Mater Res Part A* 2001;**57**:132-139.

40. Golub EE, Boesze-Battaglia K. The role of alkaline phosphatase in mineralization. *Curr Opin Orthop* 2007;**18**:444-448.

41. Bradshaw AD, Sage EH. SPARC, a matricellular protein that functions in cellular differentiation and tissue response to injury. *J Clin Invest* 2001;**107**:1049-1054.

42. Ganss B, Kim RH, Sodek J. Bone sialoprotein. *Crit Rev Oral Biol Med* 1999;**10**:79-98.

43. Hensel K, Mienkina MP, Schmitz G. Analysis of ultrasound fields in cell culture wells for in vitro ultrasound therapy experiments. *Ultrasound Med Biol* 2011;**37**:2105-2115.

44. Leskinen JJ, Hynynen K. Study of factors affecting the magnitude and nature of ultrasound exposure with *in vitro* set-ups. *Ultrasound Med Biol* 2012;**38**:777-794.

45. Petecchia L, Sbrana F, Utzeri R, Vercellino M, Usai C, Visai L *et al.* Electro-magnetic field promotes osteogenic differentiation of BM-hMSCs through a selective action on Ca^{2+}-related mechanisms. *Sci Rep* 2015;**5**:13856.

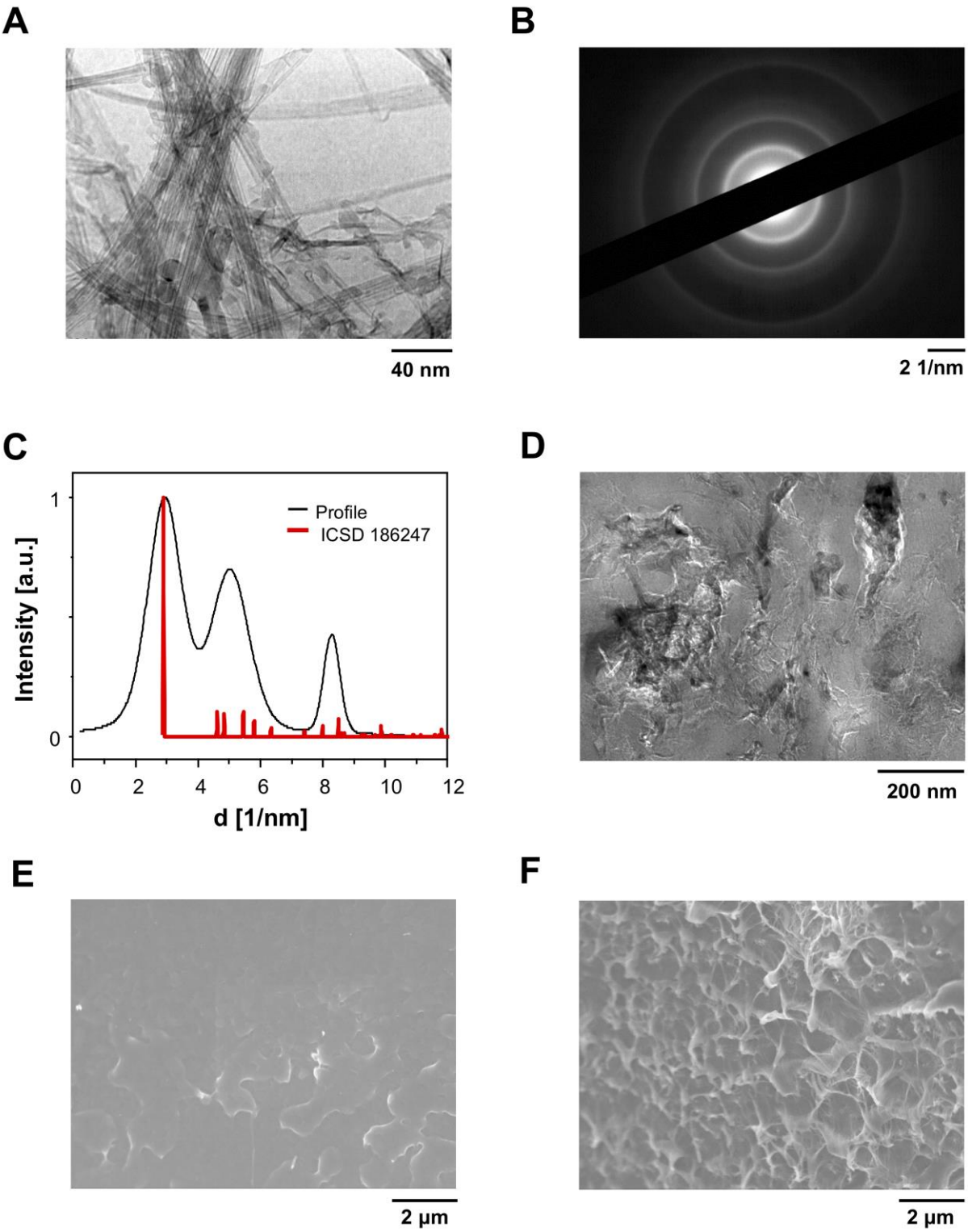
A
40 nm
B
2 1/nm
C
Intensity [a.u.]
1
0
Profile
ICSD 186247
0
2
4
6
8
10
12
d [1/nm]
D
200 nm
E
2 µm
F
2 µm

Figure 1

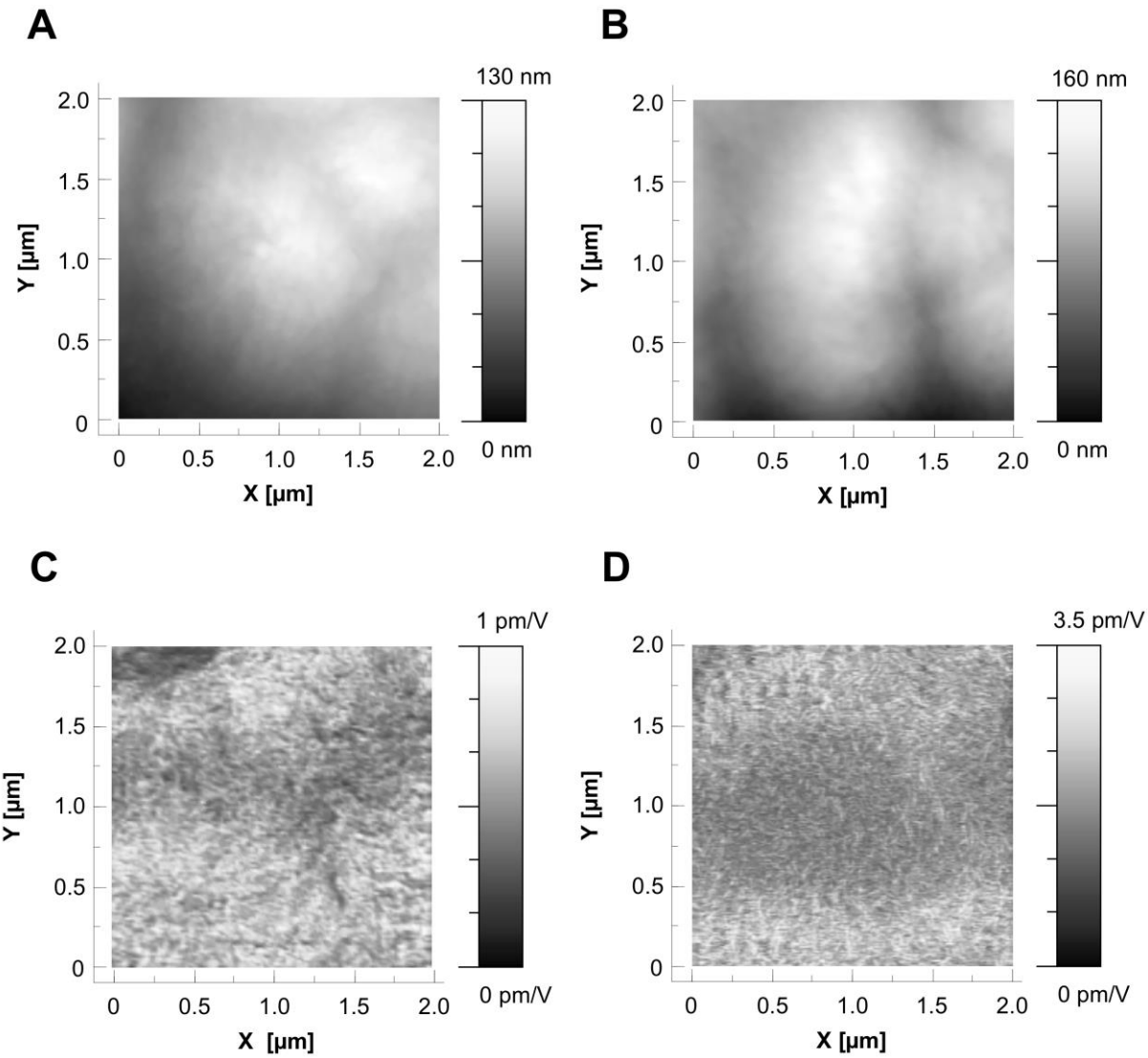

Figure 2

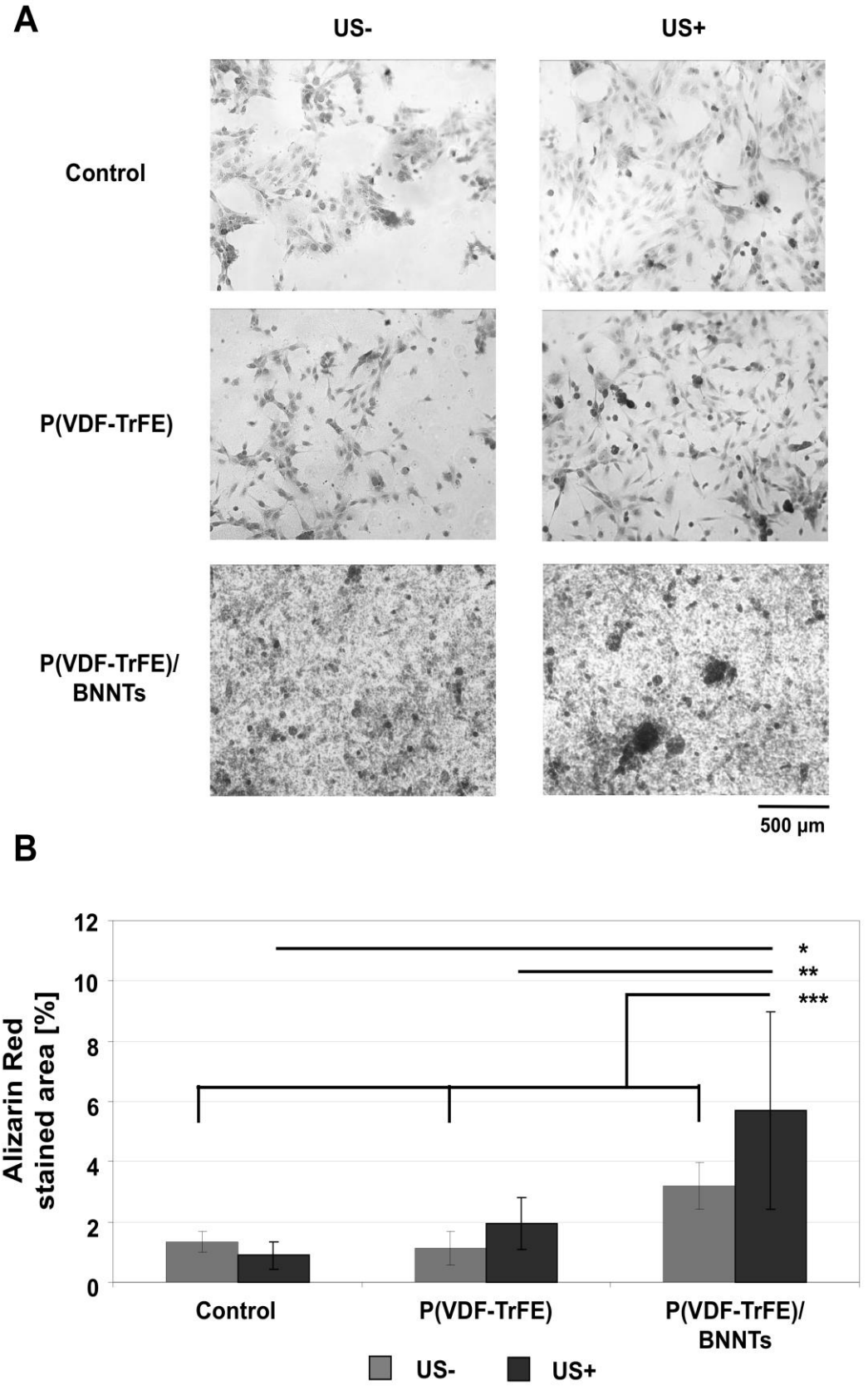
A
US-
US+
Control
P(VDF-TrFE)
P(VDF-TrFE)/
BNNTs
500 µm
B
Alizarin Red
stained area [%]
12
10
8
6
4
2
0
*
**
***
Control
P(VDF-TrFE)
P(VDF-TrFE)/
BNNTs
US-
US+

Figure 3

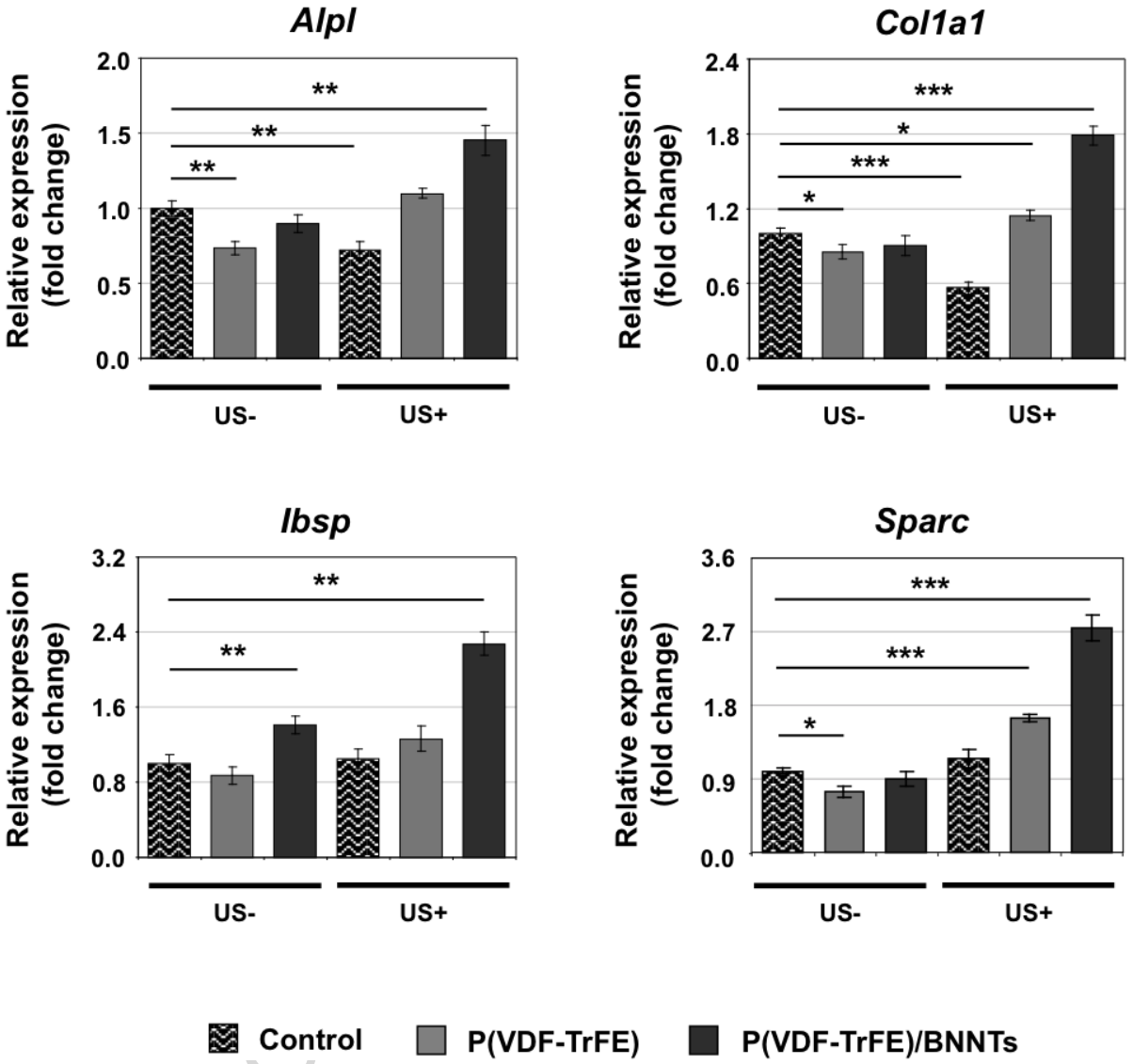

Figure 4

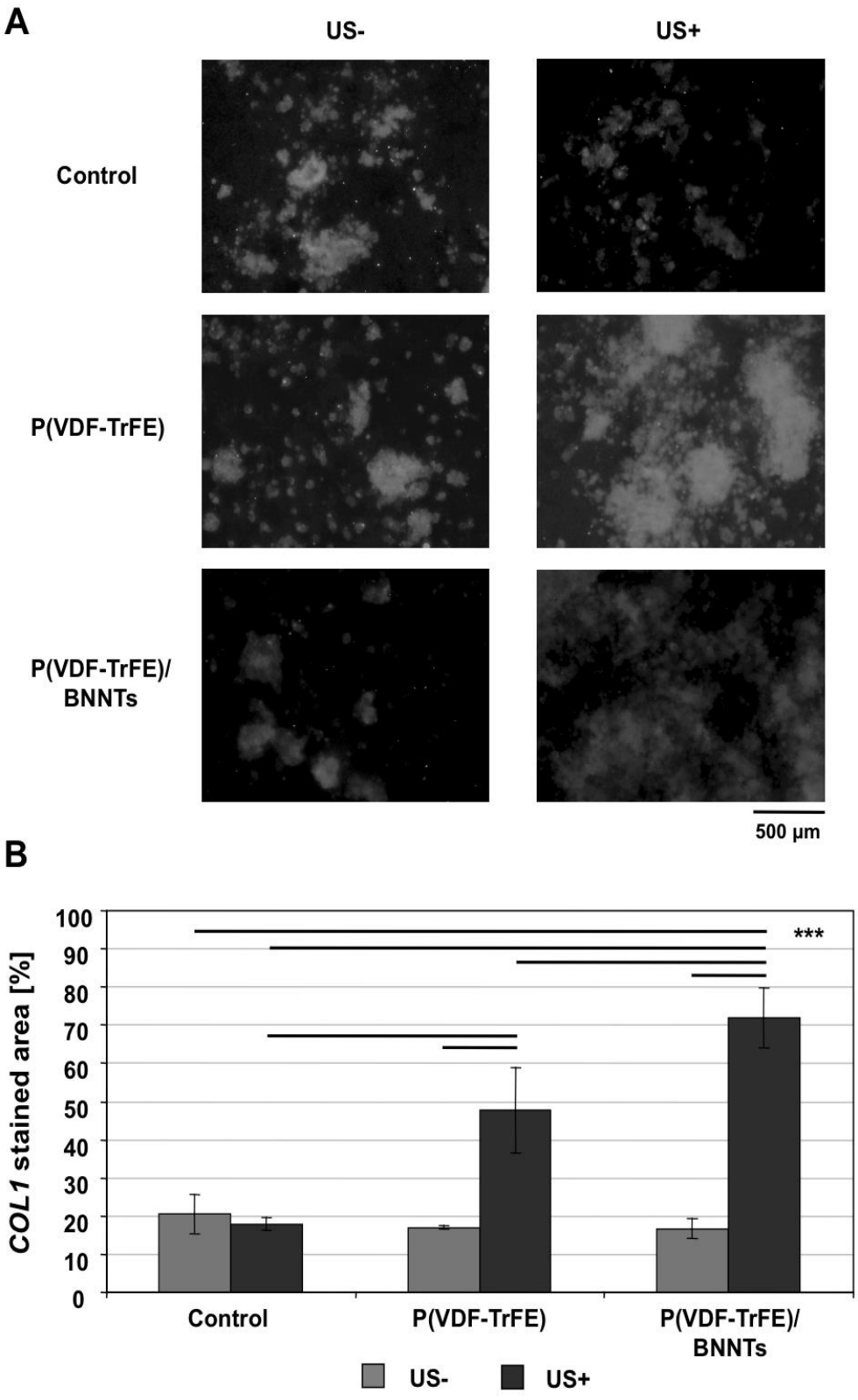
A
US-
US+
Control
P(VDF-TrFE)
P(VDF-TrFE)/
BNNTs
500 µm
B
COL1 stained area [%]
100
90
80
70
60
50
40
30
20
10
0
***
Control
P(VDF-TrFE)
P(VDF-TrFE)/
BNNTs
US-
US+

Figure 5

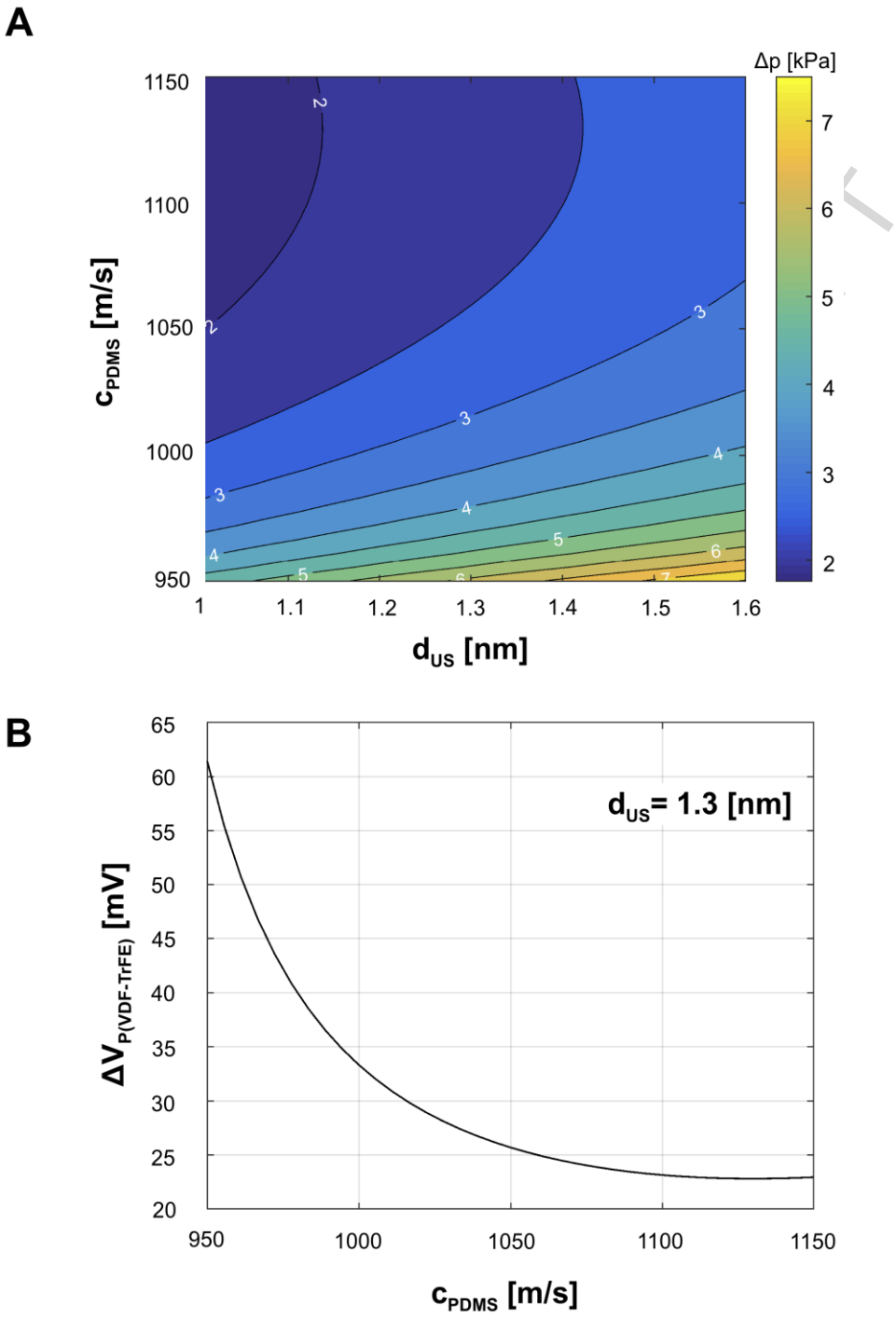
A
Δp [kPa]
7
6
5
4
3
2
1150
1100
1050
1000
950
1
1.1
1.2
1.3
1.4
1.5
1.6
c_{PDMS} [m/s]
d_{US} [nm]
B
d_{US}= 1.3 [nm]
65
60
55
50
45
40
35
30
25
20
950
1000
1050
1100
1150
$\Delta V_{P(VDF-TrFE)}$ [mV]
c_{PDMS} [m/s]

Figure 6

Graphical Abstract

Piezoelectric nanocomposite P(VDF-TrFE)/BNNTs films promote differentiation of SaOS-2 osteoblast- like cells upon ultrasounds stimulation.

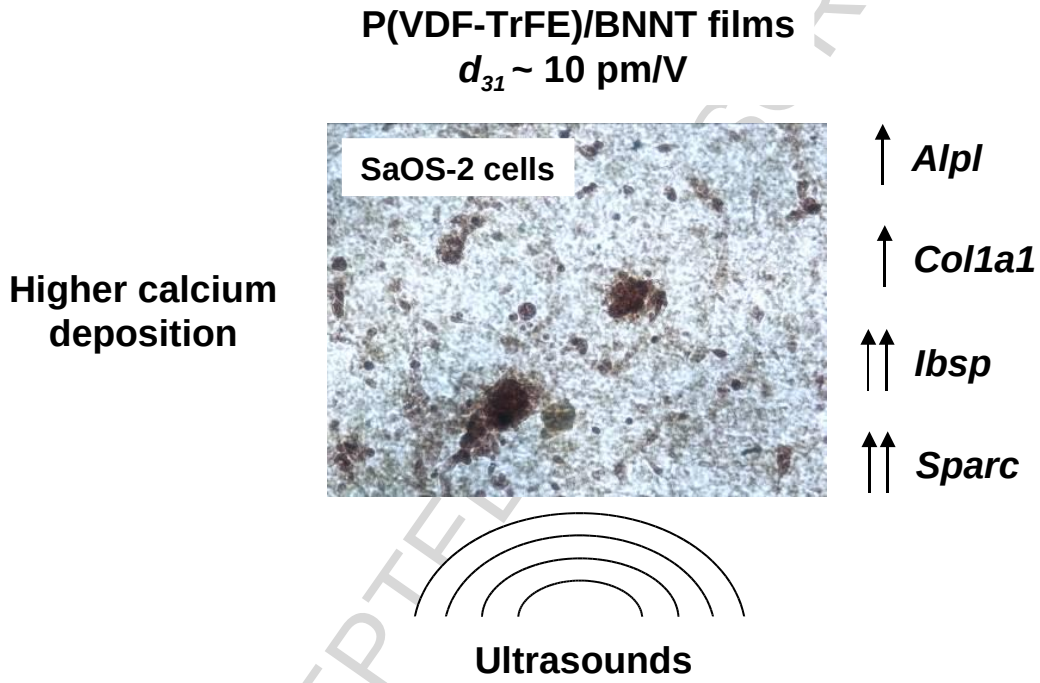

Table 1

Piezoelectric coefficient	Ibidi (negative control)	P(VDF-TrFE)	P(VDF-TrFE) / BNNTs
d_{31} [pm/V]	0.9±0.3	6±2	11±4
g_{31} [V·m /N]	0.045±0.015	0.085±0.028	0.155±0.056
e_{31} [mC/m^2]	1.31±0.57	1.92±0.83	7.59±3.52

Table 2

Material	Piezoelectric coefficient	Reference
Dry bone	0.2 pC/N (d_{31}) 0.45 pC/N (d_{33})	31
Wet bone	28 pC/N (d_{31}) 2.5 pC/N (d_{33})	31
Bone (PFM)	7.6-8.7 pC/N (d_{33})	32
Collagen from bone	0.2 pC/N ($-d_{14}$)	33
Single collagen fibril (PFM)	1 pC/N (d_{15})	34
Poled hydroxyapatite	1.8-2.5 pC/N (d_{33})	12
Poly(L-lactic acid)	9.8 pC/N (d_{14})	35
PZT	80-180 pC/N (d_{31})	36
P(VDF-TrFE)	6 pC/N (d_{31})	26
BNNTs	0.19-0.39 pC/N (d_{33})	37[#]

[#]Derived as $d_{33} = e_{33} / E_Y$ (cf. Eq. 2) based on the e_{33} values in Ref. 37, and by assuming $E_Y = 1$ TPa (cf. Refs. 16 and 17).